THE ASTROPHYSICAL JOURNAL, 328:23–33, 1988 May 1

GALAXY FORMATION WITH COSMIC STRINGS AND MASSIVE NEUTRINOS

EDMUND BERTSCHINGER AND PAUL N. WATTS
Center for Theoretical Physics, Center for Space Research, and Department of Physics, Massachusetts Institute of Technology
Received 1987 June 8; accepted 1987 October 23

ABSTRACT

We present a detailed calculation of the growth of linear density perturbations induced by a loop of cosmic string in a universe presently dominated by light massive neutrinos. The constant pulling of the cosmic string overcomes free-streaming damping so that cosmological structure develops in a "bottom-up" fashion different from hot dark matter scenarios without cosmic strings. We develop an accurate semi-analytic method for evolving the spherical perturbation around a loop through the collapse stage. Applying this method we show that halos with flat rotation curves form with circular rotation speed of ~ 50 km s^{-1} or greater. The Tremaine and Gunn phase-space constraint limits the compactness of the neutrino halos so that this scenario cannot explain dwarf spheroidals with compact dark halos. We estimate the galaxy luminosity function from the loop size distribution by applying the Faber-Jackson relation to the calculated rotation speeds and find good agreement with a Schechter function of slope $\alpha = 1.4$. For the Turok and Brandenberger loop distribution, the fit requires $\Omega h^2 \approx 1$, one neutrino flavor of mass ≈ 100 eV/c^2, and a string mass parameter $G\mu/c^2 \approx 4 \times 10^{-6}$.

Subject headings: cosmology — galaxies: formation — galaxies: internal motions — galaxies: structure — neutrinos

I. INTRODUCTION

Attention has focused recently on the idea that cosmic strings produced in the early universe may seed the formation of galaxies. Cosmic strings are massive, linear, topologically stable defects in a scalar quantum (Higgs) field which acquired a nonzero expectation value throughout most of space during a phase transition. Under some conditions the phase transition may not go to completion everywhere, leaving defects inside which the Higgs field vanishes. Cosmic strings may thus be thought of as tubes of "false vacuum"; they are analogous to magnetic flux tubes trapped in Type II superconductors. A review of their properties has been given by Vilenkin (1985).

The mass and tension of cosmic strings gravitationally perturb the ordinary matter and radiation filling the universe. These perturbations may grow to form the present structure in the universe (Zel'dovich 1980; Vilenkin 1981). Cosmic strings are hypothetical objects which, even if created in the early universe, may, like magnetic monopoles, have been diluted to negligible density by inflation (Guth 1981). Since present particle physics models are unable to decide whether cosmic strings were formed in and survived the early universe in appreciable numbers, it is important to consider their astrophysical consequences. It is amazing that cosmic strings, unlike their point-like and two-dimensional relatives, magnetic monopoles and domain walls, are not catastrophic to the evolution of structure in the universe.

Cosmic strings, like magnetic flux tubes, have no ends. Most of the string produced in a phase transition is initially in the form of infinite strings (Kibble 1976; Vachaspati and Vilenkin 1984), but as the universe expands the strings oscillate and cross themselves, breaking off closed loops (Albrecht and Turok 1985). Loops are more important than infinite strings for the subsequent seeding of structure. Turok (1985), considering a model in which galaxies form around small loops and clusters of galaxies form around large loops, showed that the clustering of large loops produced by the evolution of the string network in the early universe matches the clustering of Abell clusters as determined by the two-point correlation function (Bahcall and Soneira 1983). This discovery spurred several groups to consider galaxy formation by accretion of cold dark matter onto small loops (Sato 1986; Stebbins 1986; Turok and Brandenberger 1986). These analytic calculations showed that cosmic strings with a mass per unit length $\mu \approx (1-2) \times 10^{-6}\ c^2 G^{-1}$, a reasonable value for strings produced in the Grand Unified phase transition, can plausibly form galaxies and clusters of the correct mass and abundance.

More recent work has considered the formation of large-scale structure by cosmic strings. Shellard *et al.* (1987), Brandenberger *et al.* (1987), and Bertschinger (1988) showed that, unless μ is several times larger than the value needed to make galaxies with cold dark matter, cosmic strings are unlikely to generate large-scale streaming velocities as large as that reported by Dressler *et al.* (1987). They noted that hot dark matter (e.g., massive neutrinos) might yield better agreement since a larger μ would be required to form galaxies. Melott and Scherrer (1987), performing N-body simulations with cold dark matter, concluded that cosmic strings lead to an excessively steep correlation function. This conclusion could change if the dark matter is hot since growth is then suppressed on small scales by free-streaming damping.

In the successful standard model for galaxy formation without cosmic strings (see Blumenthal *et al.* 1984 for a review), the dark matter is postulated to be made up of some kind of cold, collisionless particle. Light massive neutrinos or other hot dark matter particles are unsatisfactory because the large thermal velocities of the particles erase galaxy-scale primordial density perturbations (Bond and Szalay 1983). Cosmic strings, by continually pulling on the matter, may ease this problem of free-streaming damping.

In this paper we consider the linear and nonlinear evolution of cosmic string-induced perturbations in a universe presently dominated by hot dark matter. For definiteness we take the dark matter to be made of one flavor of massive neutrino, e.g., ν_τ, with the other flavors being much lighter. To account for

free-streaming damping it is necessary to employ a treatment based on the neutrino phase space distribution. We do not use full general relativity but rather follow the pioneering work of Gilbert (1966) in solving the nonrelativistic Vlasov equation. Of course, some relativistic effects are important and so we include the gravitational effect of radiation and also account for the isocurvature suppression of perturbation growth outside the horizon of a string loop (Traschen, Turok, and Brandenberger 1986). The linear perturbation theory of hot dark matter and cosmic strings is presented in § II. Approximate treatments of this problem have been given by Vilenkin and Shafi (1983) and Sato (1986) (see also Schramm and Vittorio 1985); a treatment similar to ours has been presented recently by Brandenberger, Kaiser, and Turok (1987).

Linear perturbation theory shows that free-streaming damping retards, but does not eliminate, the growth of density perturbations close to the cosmic string loop. Of course, the real test of the model is whether nonlinear collapse will produce galaxies of the correct abundance and properties. The infall onto loops is, to a good approximation, spherically symmetric (neglecting the peculiar motions of loops; see Bertschinger 1987) and can be described accurately using a nonlinear "turnaround" model (Gunn and Gott 1972; Gunn 1977; Hoffman and Shaham 1985; Hoffman 1987). In this model the Zel'dovich (1970) approximation is used to evolve the density perturbation until Lagrangian shells stop expanding. Each shell is assumed then to collapse and virialize. In most treatments of this sort the shells are assumed to remain (on average) at about half of their turnaround radius, but in the present case the matter falling in later drags the preceding shells further in. We introduce an approximate model based on adiabatic invariants to account for this, and we show in § III that the method produces nonlinear density profiles accurate to within 10% for the spherical similarity solutions of Fillmore and Goldreich (1984) and Bertschinger (1985).

In § IV we apply the spherical nonlinear model to the collapse of hot dark matter onto cosmic strings. Because the linear density profiles are shallower than $\delta \propto r^{-2}$, the nonlinear collapse produces flat rotation curves (Hoffman and Shaham 1985). The results are encouraging, so we consider limitations imposed by the Tremaine and Gunn (1979) phase-space constraint, loop decay, baryonic infall, and loop motion. Using a simple model we then calculate the galaxy luminosity function.

We present our conclusions and suggest further theoretical and observational tests in § V.

It has been suggested recently that cosmic strings may, in some particle physics models, be superconducting (Witten 1985) and may form galaxies through electromagnetic interactions (Ostriker, Thompson, and Witten 1986). In this paper we assume that the strings are not superconducting or, if they are, that they carry negligible currents.

II. LINEAR PERTURBATION THEORY

In this section we derive an integral equation for the growth of small density perturbations in a collisionless gas of massive neutrinos. This equation is then solved numerically to provide initial conditions for the nonlinear collapse calculations presented in § IV.

a) *Assumptions and Derivations of the Integral Equation*

We assume that there exist two flavors (e.g., ν_e, ν_μ) of neutrinos which are light enough (with mass <1 eV/c^2) to be relativistic throughout the radiation-dominated era. A third flavor (e.g., ν_τ) has mass $m = 96.8\ \Omega h^2 \mathrm{eV}/c^2$, sufficient to close the universe ($\Omega = \rho/\rho_{\rm crit} = 1$) for a microwave background temperature of 2.7 K and Hubble constant $H_0 = 100h$ km s^{-1} Mpc^{-1} (Davis *et al.* 1981). We neglect the baryonic contribution to the density.

We consider the growth of dark matter perturbations around a single loop of string, which we treat as a stationary point of mass M_s. We use nonrelativstic Newtonian mechanics, modified for the gravitation of radiation and the suppression of growth outside the horizon of the loop. The latter effect arises because the energy density perturbations of cosmic strings are compensated by an underdensity in radiation on scales outside the causal horizon (Traschen *et al.* 1986). A nonrelativistic treatment of the massive neutrinos is justified because the neutrinos become nonrelativistic in the radiation-dominated era before significant perturbation growth occurs.

The massive neutrino velocity distribution function $f(\boldsymbol{r}, \boldsymbol{v}, t)$ satisfies the Vlasov equation

$$\frac{\partial f}{\partial t} + \boldsymbol{v} \cdot \frac{\partial f}{\partial \boldsymbol{r}} - (\nabla\phi) \cdot \frac{\partial f}{\partial \boldsymbol{v}} = 0 , \tag{1}$$

where the gravitational potential ϕ solves the Poisson equation

$$\nabla^2\phi = 4\pi G[\rho_m + 2\rho_r + M_s\delta^3(\boldsymbol{r})] . \tag{2}$$

The gravitating mass includes the massive neutrinos, with mass density $\rho_m = m\int d^3v f$, radiation consisting of the microwave background and the relativistic neutrinos, and the cosmic string. Because the radiation Jeans length is approximately the horizon distance, radiation perturbations do not grow significantly within the horizon; outside the horizon they simply cancel the string perturbation. Radiation energy density perturbations are therefore neglected.

It is convenient to transform to comoving coordinates and a new time variable:

$$\boldsymbol{x} = \frac{1}{a}\boldsymbol{r} , \quad \boldsymbol{u} = a\left(\boldsymbol{v} - \frac{\dot a}{a}\boldsymbol{r}\right), \quad s = \int^t \frac{dt}{a^2} , \tag{3}$$

where the expansion factor $a(t)$ is normalized to unity at the present time and a satisfies the Friedmann equation $(\dot a/a)^2 = (8\pi/3)G\rho_b$ ($\rho_b c^2$ is the total background energy density, including matter and radiation). With the two flavors of relativistic neutrinos the universe became matter-dominated at a redshift $1 + z_{\rm eq} = a_{\rm eq}^{-1} = 2.887 \times 10^4 h^2$. Defining the length scale $r_{\rm eq} \equiv \frac{2}{3}cH_0^{-1}a_{\rm eq}^{1/2} = 11.76h^{-2}$ Mpc, we integrate the Friedmann equation and the equation defining $s(t)$ to obtain

$$\frac{a(t)}{a_{\rm eq}} = \frac{\xi(\xi+6)}{9} , \quad \frac{ct}{a_{\rm eq}r_{\rm eq}} = \frac{\xi^2(\xi+9)}{27} ,$$
$$s = -\frac{3}{2}\frac{r_{\rm eq}}{a_{\rm eq}c}\ln\left(1 + \frac{6}{\xi}\right), \tag{4}$$

where ξ is the dimensionless conformal time:

$$\xi \equiv \frac{c}{r_{\rm eq}}\int_0^t \frac{dt}{a(t)} = 3\left[\left(1 + \frac{a}{a_{\rm eq}}\right)^{1/2} - 1\right]. \tag{5}$$

Substituting equations (2) and (3) into the Vlasov equation (1) yields

$$\frac{\partial f}{\partial s} + \boldsymbol{u}\cdot\frac{\partial f}{\partial \boldsymbol{x}} + a\left[4\pi G\rho_0\psi - \frac{GM_s}{|\boldsymbol{x}|^2}\theta(r_{\rm eq}\xi - x)\boldsymbol{e}_r\right]\cdot\frac{\partial f}{\partial \boldsymbol{u}} = 0 . \tag{6}$$

The Heaviside function $\theta(r_{eq}\xi - x)$ is introduced to suppress growth outside the causal horizon $x = r_{eq}\xi$. The present matter density ρ_0 equals, by assumption, the critical density $3H_0^2/(8\pi G)$. The mean neutrino comoving displacement ψ is defined so that the density perturbation (not necessarily small) is

$$-\nabla_x \cdot \psi = \frac{a^3\rho_m}{\rho_0} - 1 . \tag{7}$$

This comoving displacement is similar to the Lagrangian displacement field used in the treatment of cold dark matter (Bertschinger 1987). In the latter case the trajectory of a particle is $r(x, t) = a(t)(x + \psi)$, where x is interpreted as a Lagrangian coordinate. For small displacements the Lagrangian treatment is equivalent to the Eulerian treatment used here. In the present case the trajectory $a(x + \psi)$ applies not to individual neutrinos but rather to the average of many neutrinos in a small volume.

To solve equation (6), the distribution function is first linearized, $f = f_0(u) + f_1(x, u, s)$, with $|f_1| \ll f_0$. The unperturbed distribution function is a nonequilibrium Fermi-Dirac distribution (Weinberg 1972)

$$f_0 = 2\left(\frac{m}{h_P}\right)^3 (e^{u/u_0} + 1)^{-1} , \tag{8}$$

where h_P is Planck's constant, $u_0 = k_B T_{\nu 0}/(mc) = 0.514h^{-2}$ km s^{-1}, and $T_{\nu 0} = 2.7(4/11)^{1/3}$ K. The factor of 2 accounts for left-handed neutrinos and antineutrinos; the argument of the exponential is proportional to the neutrino momentum because the neutrinos decoupled while relativistic.

Fourier transforming equation (6) yields

$$\frac{\partial \hat{f}_1}{\partial s} + i(k \cdot u)\hat{f}_1 + i4\pi \frac{Ga}{k}\frac{\partial f_0}{\partial u}\left\{m\int d^3u\hat{f}_1 + M_s\left[1 - \frac{\sin(kr_{eq}\xi)}{kr_{eq}\xi}\right]\right\} = 0 , \tag{9}$$

where

$$\hat{f}_1(k, u, s) = \int d^3x e^{-ik\cdot x} f_1(x, u, s) .$$

Integrating equation (9) gives

$$\hat{f}_1 = -i4\pi \frac{G}{k}\frac{\partial f_0}{\partial u}\int_{-\infty}^{s} ds' a' e^{-i(k\cdot u)(s-s')}\left\{m\int d^3u\hat{f}_1 + M_s\left[1 - \frac{\sin(kr_{eq}\xi')}{kr_{eq}\xi'}\right]\right\} . \tag{10}$$

Equation (10) may be simplified by integrating over velocity. Integrating by parts and using equations (4) yields

$$\delta_k(\xi) = \int_0^{\xi} d\xi' \ln\left(\frac{1 + 6/\xi'}{1 + 6/\xi}\right) F[kx_{fs}(\xi', \xi)] \times \left[\delta_k(\xi') + 1 - \frac{\sin(kr_{eq}\xi')}{kr_{eq}\xi'}\right] . \tag{11}$$

The Fourier transformed density perturbation is $\delta_k = (m/M_s)\int d^3u\hat{f}_1$; a factor of M_s/ρ_0 has been absorbed into the definition of δ_k so that equation (11) is correct for any mass M_s. The function $F(x)$ is the Fourier transform of the Fermi-Dirac distribution, normalized so that $F(0) = 1$. It may be defined by the series expansion

$$F(x) = \frac{4}{3\zeta(3)}\sum_{n=1}^{\infty}(-1)^{n+1}\frac{n}{(n^2 + x^2)^2} , \tag{12}$$

where $\zeta(3) \approx 1.202$ is the Riemann ζ function. For large argument F has the asymptotic expansion $3\zeta(3)F(x) \approx x^{-4}(1 + x^{-2} + 3x^{-4} + 18x^{-6} + \cdots)$. The neutrino free-streaming distance x_{fs} is the comoving distance a neutrino with comoving velocity u_0 travels between conformal times ξ' and ξ:

$$x_{fs}(\xi', \xi) = \alpha r_{eq}\ln\left(\frac{1 + 6/\xi'}{1 + 6/\xi}\right), \quad \alpha = \frac{3}{2}\frac{k_B T_{\nu 0}(1 + z_{eq})}{mc^2} = 0.07433 . \tag{13}$$

The smallness of the coefficient α demonstrates that treating the massive neutrinos as nonrelativistic throughout the period of significant perturbation growth is a good approximation.

b) *Numerical Solution of the Integral Equation*

Equation (11) is a Volterra integral equation of the second kind and may be solved using the trapezoidal rule. The equation couples the present value of δ_k with all past values and thus requires an iterative solution. We used $\ln \xi$ as the integration variable and chose a step size $\Delta \ln \xi = 0.03$ starting at $\xi = 10^{-4}$. Successive refining of $\Delta \ln \xi$ indicated that our results are accurate to better than 0.1%.

Figure 1 shows our results for the linear growth of several Fourier components of the density perturbation. There are several features to note. First, all waves grow rapidly for $kr_{eq}\xi < 1$, when the wavelength is smaller than the horizon size. Although it appears that there is growth outside the horizon, in fact, there is no growth in physical space for $x > r_{eq}\xi$. Long waves grow because part of the wave is within the horizon. Once waves come entirely within the horizon, they suffer from neutrino free-streaming damping as long as $kx_{fs}(\xi,\infty) \gtrsim 1$. This results in the slight oscillations of the waves entering the horizon and their depressed growth evident in Figure 1 for high wavenumbers. Finally, once the free-streaming distance grows to exceed the wavelength, the waves grow in proportion to the expansion factor, or $\delta_k \propto \xi^2$ in the matter dominated era ($\xi \gg 1$).

The most interesting result shown by Figure 1 is that free-streaming damping only retards, but never reverses, the growth of string-induced perturbations. This is in marked contrast to the evolution of primordial matter perturbations without cosmic strings to drive growth (Bond and Szalay 1983), where neutrino free-streaming damping effectively erases structure on scales smaller than superclusters of galaxies. In that scenario galaxy formation proceeds in a "top-down" manner from pancake fragmentation (Doroshkevich *et al.* 1980); the resulting large-scale structure distribution does not resemble the real universe (White, Frenk, and Davis 1983). For this reason neutrinos have fallen into disfavor as a dark matter candidate, despite their being the only proposed candidate known to exist. As Figure 1 suggests and later results will confirm, light massive neutrinos can be resurrected to form galaxies in a "bottom-up" scenario with cosmic strings.

Figure 2 shows δ_k plotted against comoving wavenumber at several times. The sluggish growth in the presence of free-streaming damping produces the k^{-4} behavior evident for $kx_{fs} > 1$ ($kr_{eq} \gtrsim 50\xi$ for $\xi \gg 1$); without the cosmic string δ_k

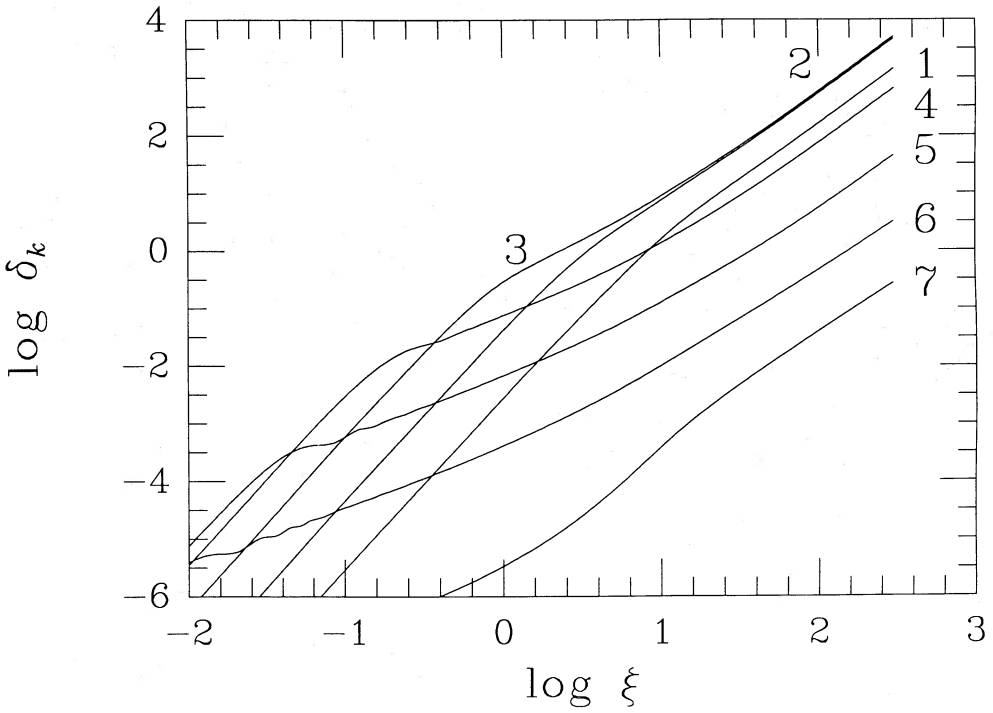

FIG. 1.—The growth of several Fourier components of the spherical hot dark matter density perturbation around a cosmic string. The abcissa ξ is dimensionless conformal time; the universe becomes matter-dominated at $\xi \approx 1$. The curves are labeled in increasing order of comoving wavenumber: $kr_{eq} = 0.398$, 1.59, 6.31, 25.1, 100, 398, and 1590. Free-streaming damping retards the growth of curves 4–7.

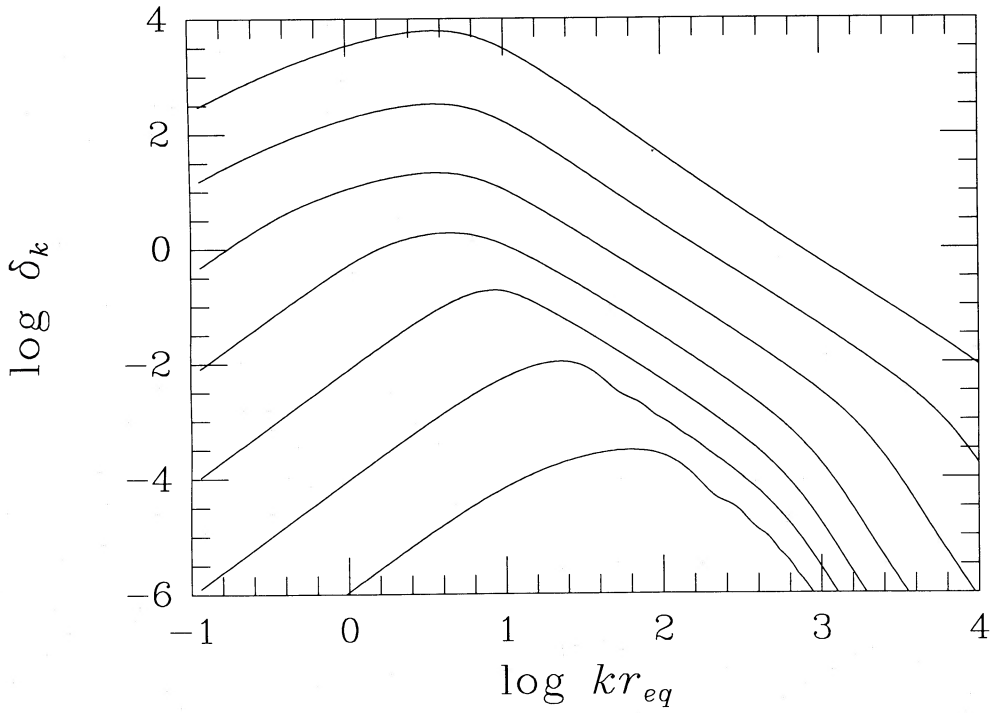

FIG. 2.—The Fourier transform of the density perturbation vs. comoving wavenumber, at conformal times $\xi = 0.031$, 0.173, 0.770, 3.42, 15.2, 67.5, and 300. Free-streaming damping creates a power-law suppression at large k.

would vanish exponentially for $kx_{fs} \gtrsim 1$. The maximum of δ_k occurs at the horizon scale (or the horizon at t_{eq}, for $\xi \gg 1$); for smaller k, $\delta_k \propto k^2$. For $\delta_k < 1$ the growth is driven primarily by the cosmic string so that the perturbation profile changes as new shells come within the horizon. Also, growth is inhibited by the dominance of radiation (Mészáros 1974) for $\xi < 1$. For $\delta_k > 1$ the matter perturbation is large enough for gravitational instability to take over (see eq. [11]), so that the profile retains the same shape (for $kx_{fs} < 1$) in the linear regime. Between the peak and x_{fs}^{-1} the density perturbation decreases (roughly as k^{-2}) because smaller wavelengths experience a smaller period of uninhibited growth after their size exceeds x_{fs}.

Figure 3 graphs the density perturbation in physical space, obtained by Fourier transforming δ_k. The perturbation is normalized to a cosmic string mass $M_s = \rho_0 r_{eq}^3 = 4.513 \times 10^{14}\ M_\odot$; for different masses δ should be multiplied by $M_s/(\rho_0 r_{eq}^3)$. Of course, the results are valid only for $\delta \ll 1$. The results also break down for $\xi < \alpha = 0.07433$, when the neutrinos are relativistic. Between the time the neutrinos become nonrelativistic and the time the perturbations become nonlinear the results should be accurate.

As is evident from Figure 3 for $\xi < 1$, the density perturbation vanishes outside the causal horizon $x/r_{eq} = \xi$. The radius of the perturbation expands with the horizon until $\xi \approx 1$, after which time the density perturbation becomes self-gravitating and retains the same shape outside the region affected by free-streaming damping. Beyond $x = 0.52 r_{eq} = 6.1 h^{-2}$ Mpc the density perturbation changes sign. This sign change seems to violate one's intuition that the cosmic string should cause the density perturbation to grow everywhere, but it has a simple explanation. The cosmic string decelerates close mass shells more than distant mass shells, so that there can be an actual thinning out of shells, hence a negative density perturbation. All shells within the horizon are, in fact, decelerated by the cosmic string.

Free-streaming damping causes the density perturbation to be uniform inside approximately $0.05 x_{fs}$. Note that despite damping, the density perturbation grows in the center. Presumably this occurs because the cosmic string traps slow-moving neutrinos even as faster ones stream away. We would thus expect a different velocity distribution close to the accreting mass, although we have not verified this by integrating equation (10). Outside the core the linear density profile varies as x^{-n}, with $n \approx 1.25$ to 1.

Simple arguments explain the form of the perturbation growth in the matter-dominated era. For $x \gg x_{fs} \approx 6\alpha r_{eq}/\xi$, the fractional mass perturbation due to the cosmic string is $3M_s/(4\pi\rho_0 x^3)$. This perturbation grows with the expansion factor $\propto \xi^2$ once x_{fs} becomes smaller than x. Thus, very roughly, we have the density perturbation (with dependence on M_s restored) growing as

$$\frac{\rho_0 r_{eq}^3}{M_s}\,\delta(x,\xi) \approx \frac{1}{3}\left(\frac{x}{r_{eq}}\right)^{-3}\left(\frac{\xi x}{r_{eq}}\right)^2 = \left(\frac{1}{3}\right)\left(\frac{x}{r_{eq}}\right)^{-1}\xi^2\,, \qquad \frac{x}{r_{eq}} \gtrsim \frac{1}{50\xi}\,. \quad (14)$$

The numerical coefficients have been chosen to give rough agreement with Figure 3 (to within about a factor of 2) for $\xi \gtrsim 10$. We see that free-streaming damping naturally produces an x^{-1} density profile.

Vilenkin and Shafi (1983) gave a rough derivation of the power spectrum of fluctuations in a universe dominated by hot dark matter with cosmic string seeds, but their results are not

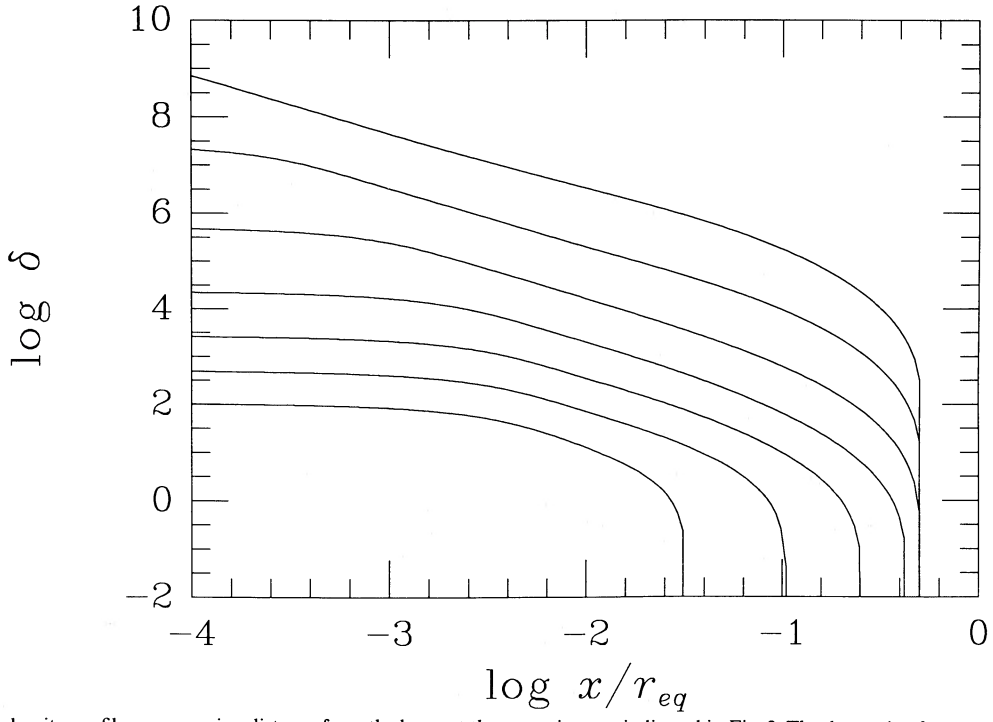

FIG. 3.—Perturbed density profile vs. comoving distance from the loop, at the same times as indicated in Fig. 2. The decreasing free-streaming distance is evident in the rise of the central density with time.

directly comparable with those obtained here because they considered a distribution of loops rather than a single loop. However, we have in essence applied their scaling arguments to a single loop in the heuristic discussion presented above and we expect a distribution of our loop perturbation solutions to yield a power spectrum qualitatively similar to theirs.

III. NONLINEAR COLLAPSE: SPHERICAL INFALL MODEL

In this section we present a method for evolving the dark matter linear perturbations computed in § II through the epoch of collapse and galaxy formation. The method we develop may be useful in other scenarios so we give a full presentation before applying it in § IV to cosmic strings and hot dark matter. One way of studying nonlinear collapse is to use an N-body code, either spherical or three-dimensional. Instead, we have chosen to follow a semi-analytic method based on spherical infall (Gunn and Gott 1972; Gunn 1977; Hoffman and Shaham 1985). Hoffman (1987) has shown that this method yields galaxy rotation curves which agree well with the results of N-body codes. We present our own comparison with exact nonlinear results below. We first review the method and then present a more sophisticated treatment which yields excellent agreement with exact calculations.

We assume that free-streaming damping is unimportant by the time nonlinear collapse begins, so that we may treat the dark matter as being effectively cold. We also neglect the orbital angular momentum of the neutrinos. These approximations are poor in the cores of the bound objects, where the neutrinos also become mildly degenerate; we will estimate below where the cold spherical results break down. Given a cold collisionless system, we may use the Lagrangian description pioneered by Zel'dovich (1970) to extend the linear perturbation theory into the initial nonlinear regime. Considering $\boldsymbol{x}$ now as a Lagrangian coordinate, the trajectory of a mass shell is $\boldsymbol{r} = a(\boldsymbol{x} + \boldsymbol{\psi})$, where $\nabla_x \cdot \boldsymbol{\psi} = -\delta$ in the linear regime. We extend this trajectory until the shell ceases expanding, $dr/dt = 0$ at $t = t_{\rm ta}$. In the matter-dominated era the turnaround time t_{ta} is then given as a function of x or, equivalently, $x_{\rm ta} = x(t_{\rm ta})$, through

$$\int_0^{x_{\rm ta}} x^2\, dx\, \delta(x, t) = \frac{1}{2}\, x_{\rm ta}^3 . \tag{15}$$

The Zel'dovich approximation thus predicts turnaround occurs when the mean density perturbation implied by linear theory is 1.5. The turnaround radius is predicted to be $r_{\rm ta}(t) = \frac{1}{2}a(t)x_{\rm ta}(t)$; the exact result is larger by a factor $(3\pi/4)^{-8/9}(12)^{1/3} = 1.069$. The Zel'dovich method works satisfactorily for following shells up to the point of turnaround.

The conventional wisdom is that, after a shell turns around, it collapses approximately a factor of 2 in radius to achieve virial equilibrium (Gunn 1977). The particles orbit about the center of the bound object, but since they spend most of the time near apoapse (the maximum orbital radius), the mass profile may be computed approximately by freezing the shells at a radius $\frac{1}{2}r_{\rm ta}$ after turnaround. This yields the virialized mass profile implicitly through

$$M = \frac{4\pi}{3}\, \rho_0\, x_{\rm ta}^3 , \quad r = \frac{1}{4}\, a x_{\rm ta} . \tag{16}$$

As demonstrated by Hoffman (1987), equation (16) yields mass profiles in good agreement with N-body simulations (Quinn, Salmon, and Zurek 1986), at least for $d \ln x_{\rm ta}/d \ln t < \frac{1}{3}$. (Hoffman actually used the exact turnaround radius.) However, for $d \ln x_{\rm ta}/d \ln t > \frac{1}{3}$ or $d \ln \delta/d \ln x > -2$, equation (16) predicts rising rotation curves while N-body simulations show nearly flat rotation curves (Frenk *et al.* 1985). Hoffman and Shaham (1985) noted that this flattening was to be expected from the results of Fillmore and Goldreich (1984), who obtained analytic similarity solutions for collisionless infall. Unfortunately, no simple modification of equation (16) can give the virialized mass distribution for $d \ln \delta/d \ln x > -2$, since shells falling in later drag in shells which fell in earlier so that the inner mass profile is not static. Since the linear density profiles found in § II have $d \ln \delta/d \ln x \approx -1$, similar to cold dark matter without cosmic strings, a more complicated dynamical model is required here.

To improve the simple turnaround model we present a method based on the adiabatic invariance of the action as the mass grows by secondary infall. Basically we extend the asymptotic analysis of Fillmore and Goldreich (1984) out to the turnaround radius. The method is similar to that used by Gunn (1977) except that we allow the halo to shrink indefinitely if required by infall. For a particle executing radial orbits in a mass distribution $M \propto r^\gamma$ which varies slowly in time compared to the orbital period, the action is (Fillmore and Goldreich 1984).

$$S = 4\int_0^{r_a} dr\left(\frac{dr}{dt}\right) = 4(2GM_a r_a)^{1/2}\int_0^1 ds\left(\frac{1 - s^{\gamma-1}}{\gamma - 1}\right)^{1/2} , \tag{17}$$

where M_a is the mass interior to the apoapse radius r_a. Neglecting the small changes in the integral involving γ, we conclude that $M_a r_a$ is an adiabatic invariant. This is also true for circular orbits, where the angular momentum is conserved.

To find the mass profile, we compute how M_a changes for a given particle as a result of secondary infall. The invariance of $M_a r_a$ then gives us the mass profile $M_a(r_a)$. We make the approximation that the orbital period is much less than the age t for all particles which have turned around by time t, so that the adiabatic invariance holds throughout the turnaround region. It is clear that this assumption breaks down near $r_{\rm ta}(t)$, but we proceed nevertheless. We will show that the resulting errors are not large.

Given the approximations stated above, the mass enclosed by r_a for a fixed particle labeled by x increases as

$$\frac{\partial M_a(x, t)}{\partial t} = 4\pi\rho_0\, x_{\rm ta}^2\, \frac{dx_{\rm ta}}{dt}\, P\left[\frac{r_a(x, t)}{r_{\rm ta}(t)}\right] , \tag{18}$$

where P is the fraction of time a particle turning around at time t spends inside r_a. For a nonsingular potential $P(x) \propto x$ for $x \ll 1$; we make the *Ansätz* $P(x) = \frac{1}{6}x$ and apply this for all $x < 1$. This assumption is clearly wrong near $x = 1$, but we believe that the results obtained below justify this *Ansätz*. If most of the particles turning around have large periapses because they have significant angular momentum, then $P(x)$ would have to be reduced at small x. Using the adiabatic invariance of $M_a r_a$, we obtain

$$\frac{\partial}{\partial t}\left(\frac{1}{r_a^2}\right) = \left(\frac{4}{x^4 a_i}\right)\frac{x_{\rm ta}}{a}\,\frac{dx_{\rm ta}}{dt} , \tag{19}$$

where $a_i = a_i(x)$ is the expansion factor when the given shell turns around. Equation (19) is to be solved subject to the initial condition (from the Zel'dovich approximation) $r_a(x, t) = \frac{1}{2}a_i x$

at $a(t) = a_i(x)$. The solution may be written as a quadrature:

$$\frac{a_i x}{2r_a} \equiv A(x, t) = \left(1 + \int_1^q dqq \frac{a_i}{a}\right)^{1/2}, \quad q \equiv \frac{x_{ta}(t)}{x}. \quad (20)$$

The integral is for fixed x so that $q = q(t)$. The quantity A is simply the factor by which the mass interior to the apoapse radius of the particle increases due to secondary infall. Thus, to obtain the nonlinear mass profile from the mass and radius of shells at turnaround, one simply multiplies the mass by A and the radius by A^{-1}. The shrinkage factor A can be computed once $x_{ta}(t)$ is known from equation (15). In general the integrals in equations (15) and (20) must be performed numerically.

For power-law linear density profiles $\delta(x) \propto x^{-n}$, like those considered by Fillmore and Goldreich (1984) and Bertschinger (1985), equation (20) is easily solved to give (for $n \neq 2$)

$$A = \left[\left(\frac{1-n}{2-n}\right) + \frac{1}{2-n}\left(\frac{a}{a_i}\right)^{(2/n)-1}\right]^{1/2}. \quad (21)$$

For $n > 2$ the orbits thus shrink a finite amount while for $n \leq 2$ they continue shrinking. The asymptotic mass dependence for $x \ll x_{ta}(a \gg a_i)$ is easily shown to be $M(r, t) \propto r^{3/(1+n)}$ for $n > 2$ and $M(r, t) \propto ra^{(2/n)-1}$ for $n < 2$, as found by Fillmore and Goldreich.

Figure 4 compares the mass profile derived from the turnaround model presented above with the exact profile obtained by Bertschinger (1985) for the $n = 3$ similarity solution. The dimensional mass profile was computed for each case, and then the radius was normalized by the exact turnaround radius, with the mass being scaled by $(4\pi/3)a^{-3}\rho_0 r_{ta}^3$. Inside the outer caustic the agreement is remarkable. Good agreement (with errors less than $\sim 10\%$) also obtains for the similarity solutions with $n = 2.4$, 1.5, and 0.6 presented by Fillmore and Goldreich (1984). We thus are confident, to the extent that the infall can be treated as being cold, that the modified turnaround model will give accurate rotation curves for the halos accreted by cosmic strings.

IV. GALAXY FORMATION: RESULTS

Applying the spherical nonlinear model described in § III to the linear density profiles derived in § II for cosmic strings and massive neutrinos, we have calculated the present-day rotation curves from the mass profiles: $V_c = (GM/r)^{1/2}$. The results are shown in Figure 5 for $\Omega = h = 1.0$ and several masses of cosmic string loops. The rotation curves are remarkably flat. They extend remaining flat to $\sim 20\%$ of the present turnaround radius which, even for the lightest loop shown here, exceeds 100 kpc. This result differs from that of Sato (1986), who found rising rotation curves ($\rho \propto r^{-3/2}$) because he neglected orbital shrinkage. The rotation curves would be modified at large radius by tidal interactions with neighboring galaxies, which have not been included here. This competition for matter by several loops should not affect the rotation curves well inside the tidal radius. The rotation curves are also modified at small radii by several processes which will be discussed below (§§ IV*a–b*). These modifications do not alter the conclusion that cosmic strings produce hot dark matter halos corresponding to flat rotation curves. By contrast, cold dark matter and cosmic strings yield rotation curves declining as $V_c \propto r^{-1/8}$ (Zurek 1986). We will also show (§ IV*c*) that the distribution of galaxy luminosities (as measured by V_c) in the hot dark matter model agrees reasonably well with observations.

a) The Phase-Space Constraint

A crucial consideration for hot dark matter is the phase-space density constraint of Tremaine and Gunn (1979). They pointed out that the maximum coarse-grained phase-space

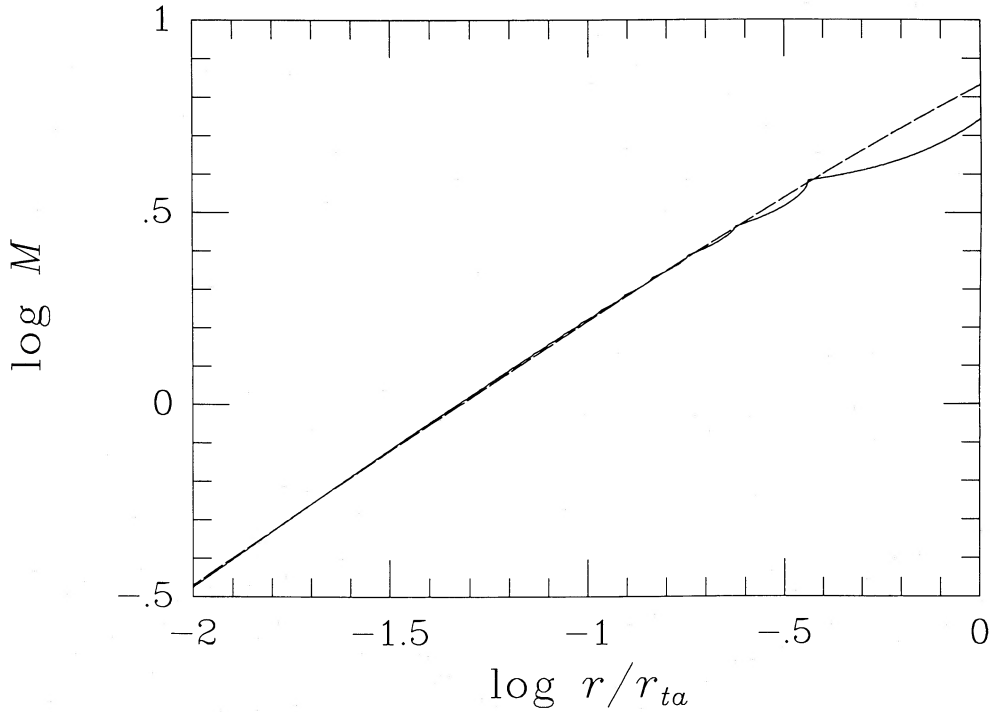

FIG. 4.—Mass profile for self-similar accretion of cold dark matter onto a point mass. Solid curve gives the exact solution while the dashed curve gives the profile obtained from the semi-analytic turnaround model described in the text.

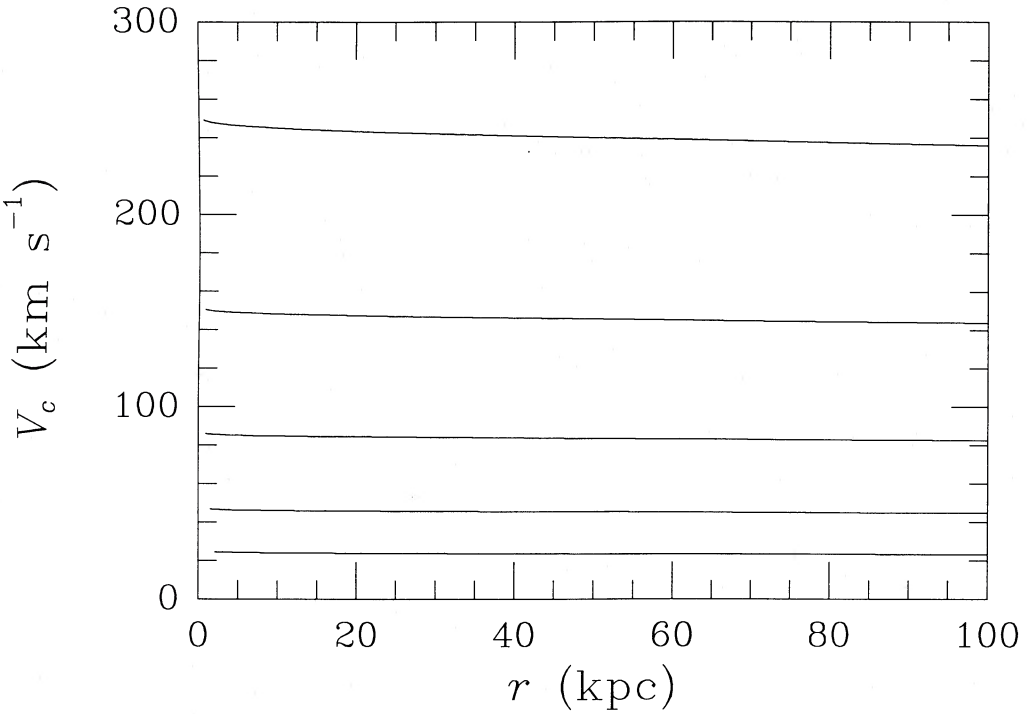

FIG. 5.—Rotation curves for the hot dark matter halos accreted by cosmic string loops of masses 1, 2, 4, 8, and $16 \times 10^8\ M_\odot$. The mass distributions were calculated using the turnaround model.

density must be less than the maximum initial fine-grained density h_P^{-3} because of phase mixing. This constraint yields, for the rotation curves of Figure 5, a minimum radius inside of which the phase space density would have to increase. In fact, this constraint has already been applied in Figure 5. The curves have been truncated at small radii so that the phase space constraint is satisfied over the entire range plotted.

To estimate the minimum halo radius we approximate the halos as singular isothermal spheres since the rotation velocity is so nearly constant for all radii. We approximate the phase-space distribution of the halo particles as Maxwell-Boltzmann. Neutrino degeneracy and the possibility of other phase space density distributions consistent with a flat rotation curve can change the results somewhat (Madsen and Epstein 1984). The phase-space constraint is then satisfied for radii r satisfying

$$r^2 V_c > \frac{h_P^3}{4\pi^{5/2} G m^4} . \tag{22}$$

This result differs by a numerical factor from that of Tremaine and Gunn (1979), who used the central density and core radius for a nonsingular isothermal sphere. For one species of neutrino dominating the mass density, equation (22) becomes

$$\left(\frac{r}{\text{kpc}}\right)^2 \left(\frac{V_c}{\text{km s}^{-1}}\right) > 73.8(\Omega h^2)^{-4} . \tag{23}$$

Because Tremaine and Gunn assumed $\Omega h^2 = 0.0125$, they concluded that light massive neutrinos cannot constitute the dark matter in galaxy halos. This is not true for $\Omega = h = 1$, although a very short age of the universe (6.5×10^9 yr) would then be implied.

Kormendy (1987) has recently summarized the observational data relating to hot dark matter in dwarf galaxies, which provide the best test of the phase space constraint. The smallest known spiral galaxy, DDO 127, has an approximately flat rotation curve beyond ~ 2 kpc with $V_c \approx 34$ km s^{-1}. This halo is consistent with equation (23). Figure 5 suggests that cosmic strings and hot dark matter can make dwarf spirals this small, although loop decay, which we discuss below, creates some difficulties.

The strongest application of the phase space constraint will come from dwarf spheroidals (Lin and Faber 1983). If these tiny galaxies contain significant amounts of dark matter, that matter cannot be light massive neutrinos. The observational status of dark matter in dwarf spheroidals is unclear. Aaronson and Olszewski (1987) find velocity dispersions of ~ 10 km s^{-1}, corresponding to $V_c \approx 14$ km s^{-1}, in the Local Group dwarfs Ursa Minor and Draco. These galaxies have visible core radii of ~ 0.15 kpc. If these measurements are confirmed by other groups and the possibility of dark baryons is excluded, we will have to dismiss the hot dark matter scenario, or at least to postulate the existence of more than one form of collisionless dark matter.

b) Loop Decay, Baryon Infall, and Loop Motion

A second process modifying the rotation curves at small radius is the decay of string loops by emission of gravitational radiation. A loop of mass M_s and mass per unit length μ decays in a time (Vachaspati and Vilenkin 1985) $t_d \lesssim M_s c/(45 G\mu^2)$. For $G\mu/c^2 = 4 \times 10^{-6}$ and $h = 1$, the lightest loop considered in Figure 5 decays by a redshift $z_d = 650$. The disappearance of the loop has little effect on mass shells with $x > x_{fs}(t_d)$ since by this time gravitational instability has already produced perturbations in the hot dark matter exceeding the direct mass perturbation of the string. For $x < x_{fs}(t_d)$ loop decay retards collapse. From these considerations we conclude that loop decay would ruin the entire bottom rotation curve shown in Figure 5 and would depress the next

lowest curve (with $V_c \approx 45$ km s^{-1}) for $r \lesssim 15$ kpc, but would have little effect on the other curves. These estimates are rough and need to be refined by redoing the linear perturbation theory with loop decay included before a reliable estimate of the minimum mass halo can be obtained. Moreover, baryonic settling may be sufficient to preserve flat rotation curves with $V_c < 50$ km s^{-1}.

Our treatment has neglected the baryonic mass component. Baryons are important because, besides producing the visible matter in galaxies, they dominate the gravitational mass in galaxy cores. Baryonic infall not only directly increases the mass inside a given radius; it also pulls in the dark matter (Blumenthal *et al.* 1986). These effects are enhanced in the case of cosmic strings because the baryon Jeans length is much less than the neutrino free-streaming damping length. Thus, even without dissipation the baryons will be pulled in more by a loop than the neutrinos will be for loops decaying after recombination at a redshift 1300. In principle, the resulting mass profiles can be calculated using the same methods as described in § III, but we will leave this for future work. These calculations would be important in establishing whether dwarf galaxies with small core radii can form with hot dark matter and cosmic strings. We can already conclude that baryons must dominate in the centers of such systems.

Finally, we have neglected the peculiar motions of the loops by treating them as stationary in the comoving frame. Loops are formed with relativistic peculiar velocities. Neglecting acceleration by beamed gravitational radiation (Vachaspati and Vilenkin 1985; Hogan 1987), the peculiar velocity of a loop decreases by the redshift factor (u = const. in eq. [3]). It is clear that the loop motion will have little effect on the dark matter if the loop moves less than the neutrino free-streaming distance. For a loop formed at expansion factor a_f with peculiar velocity v_f, loop motion can thus be neglected if $a_f v_f < u_0 = 0.514h^{-2}$ km s^{-1}. This condition implies $(1 + z_f)/(1 + z_{eq}) > 2.0(v_f/0.1c)$, or $\xi_f < 0.67$ for a typical speed $v_f = 0.1c$. Using the Turok and Brandenberger (1986) loop formation model, the mass of a loop formed at conformal time ξ_f is

$$\frac{M_s}{a_{eq}\mu r_{eq}} = \frac{\epsilon\beta}{27}\xi_f^2(\xi_f + 9)\,, \tag{24}$$

where $\epsilon \approx 0.2$ and $\beta = 9$. The neutrino streaming argument now implies that large loop formation velocities have no appreciable effect on the hot dark matter for $M_s \lesssim 1.0 \times 10^{10}h^{-4}(\mu_{-6}/4)\ M_\odot$, where $\mu_{-6} \equiv 10^6c^2/G$. Since galaxies are formed by smaller loops (see Fig. 5), we conclude that initial loop motion has no effect on the dark matter in galaxies. Loop motion would more easily affect the slower-moving baryons and could play a role if the rocket effect accelerates the loop (Hogan 1987). However, as shown by Bertschinger (1987), loop motion does not decrease the amount of mass that collapses around (or behind) the loop.

c) *Luminosity Function of Galaxies*

A successful theory of galaxy formation must not only be able to produce galaxies, it must produce them in the right numbers and sizes. In the cosmic string scenario the size distribution is fairly well determined since each loop is responsible for creating one object. Mergers can complicate this simple picture, and we will consider them briefly.

For the loop size distribution we rewrite the distribution adopted by Bertschinger (1988) using the dimensionless conformal time:

$$r_{eq}^3\, dn(\xi_f) = v\epsilon^{-3/2}\left[\frac{3(\xi_f + 6)}{\xi_f(\xi_f + 9)}\right]^4 d\xi_f\,. \tag{25}$$

This equation gives the mean number of loops in a volume r_{eq}^3 formed in the interval $d\xi_f$ about ξ_f. Turok and Brandenberger (1986) estimate $v \approx 0.01$. Obtaining the number density of loops of a given mass from equations (24) and (25), we can determine the number density of galaxies dn/dV_c of a given asymptotic circular rotation speed. We prefer to describe galaxy sizes by V_c since this quantity is fairly well determined both observationally and theoretically. Other measures, such as galaxy luminosity, depend on details of baryon collapse and star formation which are poorly understood.

To obtain the observed galaxy number-rotation speed distribution we combine the Schechter (1976) luminosity function

$$dn = \phi_*\left(\frac{L}{L_*}\right)^{-\alpha} e^{-L/L_*} d\left(\frac{L}{L_*}\right) \tag{26}$$

and the empirical luminosity-velocity dispersion relation of Faber and Jackson (1976), as measured by Sargent *et al.* (1977; corrected to $H_0 = 100h$ km s^{-1} Mpc^{-1}):

$$\log \sigma = 0.366 + 0.5 \log h - 0.100M_B\,. \tag{27}$$

For an isothermal distribution, $\sigma = 2^{-1/2}V_c$. For the Schechter function parameters, we fix $M_B^* = -19.1 + 5 \log h$ and $\phi_* = 0.012h^3$ Mpc^{-3} (Davis and Huchra 1982).

Figure 6 compares the theoretical distribution, assuming one galaxy per loop and $h = 1$, with the empirical relation. The string mass per unit length and the empirical faint-end slope α have been chosen to give the best agreement, yielding $G\mu/c^2 = 4 \times 10^{-6}$ and $\alpha = 1.38$. Measurements of α are uncertain, ranging from $\alpha = 1.25$ (Schechter 1976) to $\alpha = 1.6$ (Godwin and Peach 1977), with $\alpha = 1.38$ being consistent with most measurements. Because the Hubble constant and the parameters of the loop size distribution are uncertain, we have done the calculations for a range of parameters, from which we conclude $dn/dV_c \propto v(\beta\mu)^{3/2}h^{9/2}$. The strong dependence on h arises mostly because for smaller Hubble constant r_{eq} is larger so that the number density of loops produced near z_{eq} is smaller. Agreement with observations therefore requires

$$\frac{G\mu}{c^2} \approx 4 \times 10^{-6}h^{-3}\left(\frac{v}{0.01}\right)^{-2/3}\left(\frac{\beta}{9}\right)^{-1}\,. \tag{28}$$

We consider the faint end of the luminosity function a strong success for cosmic strings and hot dark matter with $h = 1$. A smaller Hubble constant would require more or more massive loops; microwave background isotropy limits probably require $G\mu/c^2 < 10^{-5}$ (Kaiser and Stebbins 1984). We should stress, however, that Figure 6 neglects loop decay, which might make it difficult to form galaxies with $V_c \lesssim 50$ km s^{-1} (§ IV*b*). The number density of such faint galaxies ($M_B \lesssim -12$) is poorly known.

The cosmic string model overestimates the number of massive ($V_c \gtrsim 300$ km s^{-1}) galaxies, but it is not unique in this regard. Frenk *et al.* (1985) also find overly massive halos in N-body simulations of cold dark matter. Such systems are probably actually groups of galaxies rather than galaxies. Frenk *et al.* follow only the evolution of the dark matter halos, which may merge even when the baryon cores remain intact. To an optical observer such a system is a group of galaxies

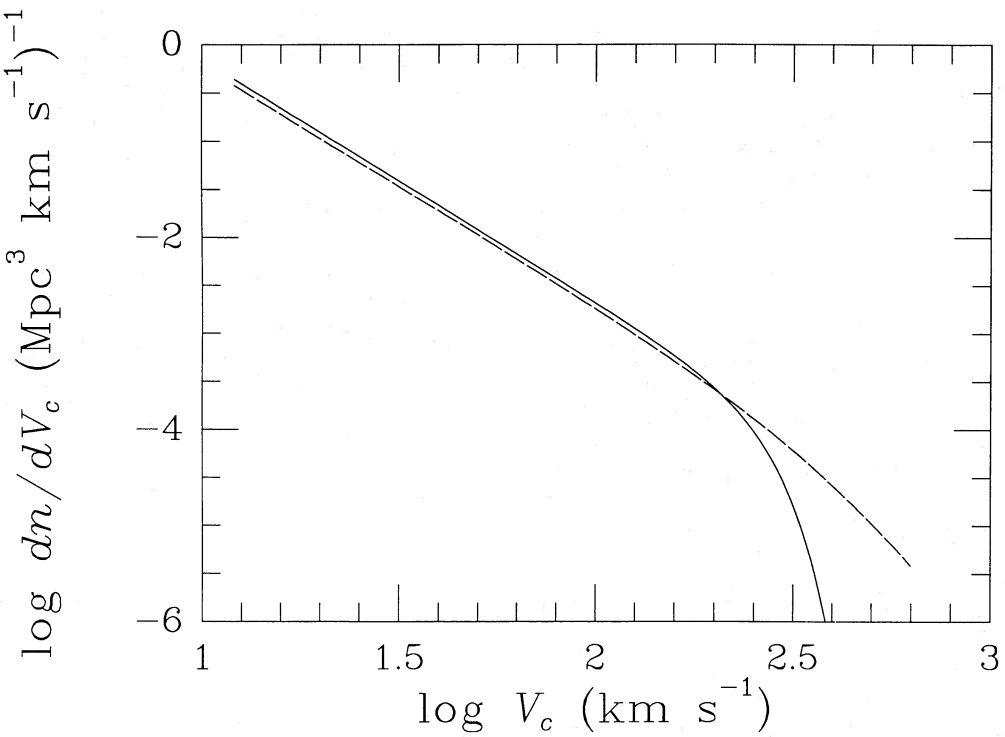

FIG. 6.—The distribution of galaxies of varying asymptotic circular rotation speeds. Solid curve corresponds to a Schechter luminosity function with slope $\alpha = 1.38$; luminosity has been converted to velocity dispersion and then to rotation speed using the Faber-Jackson relation for an isothermal halo. Dashed curve is the result of the cosmic string model with hot dark matter, $\Omega = h = 1$, and $G\mu/c^2 = 4 \times 10^{-6}$.

even though dynamically it may better be described as a single massive halo. We believe that the same interpretation applies here.

To test the importance of mergers we compared the mean separation $n^{-1/3}$ of galaxies more massive than a given size with the present turnaround radius. The turnaround radius exceeds $0.5n^{-1/3}$ for $V_c \gtrsim 150$ km s^{-1}. We argue crudely that if a galaxy merges with a lighter one it will change little, while if it merges with a more massive one it will be disrupted. This argument is not very strong, but it does suggest that mergers do not strongly modify the luminosity function for $V_c \lesssim 150$ km s^{-1}.

We conclude that the distribution of galaxy sizes looks promising in the strings and hot dark matter model, but we caution that the analytic arguments presented here should not be trusted too much. It is important that N-body simulations be performed to test these results.

V. DISCUSSION

We have considered the linear and nonlinear growth of perturbations in hot dark matter induced by loops of cosmic string. Interestingly, for $\Omega h^2 = 1$ and $G\mu/c^2 = 4 \times 10^{-6}$ the model yields flat rotation curves and good agreement with the empirical galaxy luminosity function. The large value of Ωh^2 implies an uncomfortably short universe age of 6.5×10^9 yr but is consistent with direct measurements of Ω and h.

Small values of Ωh^2 are unsatisfactory in this model for two reasons. First, the Tremaine and Gunn (1979) phase-space density constraint has the minimum hot dark matter core radius scaling as $(\Omega h^2)^{-2}$. For a neutrino mass $m \approx 100$ eV/c^2 ($\Omega h^2 = 1$) the phase-space constraint is barely satisfied for the smallest known dwarf spirals and is already violated if dwarf spheroidals with $M_B \lesssim -10$ contain significant amounts of dark matter within 1 kpc of their centers (Kormendy 1987). Second, a smaller Ωh^2 reduces the duration of the matter-dominated era and so reduces the growth of dark matter perturbations; a smaller Ωh^2 also increases the neutrino free-streaming distance. These effects require heavier or more numerous strings for compensation (eq. [28]). Microwave background isotropy constraints require $G\mu/c^2 \lesssim 10^{-5}$ (Kaiser and Stebbins 1984). For $h = 0.5$ this is consistent with galaxy formation by strings and massive neutrinos only if the Turok and Brandenberger (1986) loop distribution parameters are seriously in error, which is a possibility.

Let us suppose that cosmic strings do exist with $G\mu/c^2 = 4 \times 10^{-6}$. How can they be detected? First, gravitational lensing by strings (Vilenkin 1981) produces pairs of images with typical separation $4\pi G\mu/c^2 \approx 10''$. A large loop could lens several background quasars. The detection of several pairs of images along a curve would hint at a cosmic string (Gott 1986; Vilenkin 1986). A definitive test would come from the observation of a step-like discontinuity in the microwave background temperature. Kaiser and Stebbins (1984) showed that $\delta T/T \approx 8\pi G\mu/c^2 \approx 10^{-4}$ across a string moving relativistically transverse to the line of sight. Finally, the gravitational radiation background produced by decaying loops would introduce timing noise into millisecond pulsars which should become measurable within a few years (Hogan and Rees 1984). We conclude that cosmic strings should not be very elusive objects.

Our calculations are most uncertain in the cores of galaxies because we did not include directly neutrino phase mixing, loop decay, or baryonic infall. A more careful treatment of these effects is needed to determine the galaxy core radii. The

model is not likely to have severe problems except with dwarf spheroidals, but it would be useful to determine whether any signature of cosmic strings or massive neutrinos may be found in galaxy cores. The signature will not be as obvious as a 10^9 $M_\odot$ string loop sitting in the Galactic Center, since such a loop would have decayed at $z \gtrsim 40$. We note that after the string evaporates galaxy formation is similar to the standard cold dark matter scenario, since the neutrino free-streaming distance is then subgalactic. Although some nonlinear structure forms at $z > 100$, most of the structure forms in the last few expansion times.

Our analytic collapse calculations need to be supplemented by N-body simulations. We have shown that the Schechter (1976) luminosity function is a plausible outcome (with $\alpha = 1.4$), but we would like to see numerical confirmation of this since we neglected galaxy mergers. Also, such calculations could address the question of angular momentum generation, which we have ignored. Here loop motion might be important (Bertschinger 1987).

Finally, N-body simulations are needed to test large-scale structure formation. Melott and Scherrer (1987) found unsatisfactory results for cosmic strings and cold dark matter: the large-scale matter distribution is too lumpy. Shellard *et al.* (1987), Brandenberger *et al.* (1987) and Bertschinger (1988) found too small large-scale streaming velocities with cold dark matter. Hot dark matter is bound to be an improvement but quantitative answers will require large simulations.

In summary, we have presented some of the details of a theory of galaxy formation with cosmic strings and massive neutrinos. We find that cosmic strings solve many of the problems normally associated with hot dark matter and vice versa. As unusual as this combination may seem, it clearly deserves closer study.

We wish to thank Roman Juszkiewicz for inspiring this work and Marc Davis for several helpful suggestions.

REFERENCES

Aaronson, M., and Olszewski, E. 1987, in *IAU Symposium 117, Dark Matter in the Universe*, ed. J. Kormendy and G. R. Knapp (Dordrecht: Reidel), p. 153.
Albrecht, A., and Turok, N. 1985, *Phys. Rev. Letters*, **54**, 1868.
Bahcall, N. A., and Soneira, R. M. 1983, *Ap. J.*, **270**, 20.
Bertschinger, E. 1985, *Ap. J. Suppl.*, **58**, 39.
———. 1987, *Ap. J.*, **316**, 489.
———. 1988, *Ap. J.*, **324**, 5.
Blumenthal, G. R., Faber, S. M., Flores, R., and Primack, J. R. 1986, *Ap. J.*, **301**, 27.
Blumenthal, G. R., Faber, S. M., Primack, J. R., and Rees, M. J. 1984, *Nature*, **311**, 517.
Bond, J. R., and Szalay, A. S. 1983, *Ap. J.*, **274**, 443.
Brandenberger, R., Kaiser, N., Shellard, E. P. S., and Turok, N. 1987, *Phys. Rev. D*, **36**, 335.
Brandenberger, R., Kaiser, N., and Turok, N. 1987, *Phys. Rev. D*, **36**, 2242.
Davis, M., and Huchra, J. 1982, *Ap. J.*, **254**, 437.
Davis, M., Lecar, M., Pryor, C., and Witten, E. 1981, *Ap. J.*, **250**, 423.
Doroshkevich, A. G., Kotok, E. V., Novikov, I. D., Polyudov, A. N., Shandarin, S. F., and Sigov, Yu. S. 1980, *M.N.R.A.S.*, **192**, 231.
Dressler, A., Faber, S. M., Burstein, D., Davies, R. L., Lynden-Bell, D., Terlevich, R. J., and Wegner, G. 1987, *Ap. J. (Letters)*, **313**, L37.
Faber, S. M., and Jackson, R. E. 1976, *Ap. J.*, **204**, 668.
Fillmore, J. A., and Goldreich, P. 1984, *Ap. J.*, **281**, 1.
Frenk, C. S., White, S. D. M., Efstathiou, G., and Davis, M. 1985, *Nature*, **317**, 595.
Gilbert, I. H. 1966, *Ap. J.*, **144**, 233.
Godwin, J. C., and Peach, J. V. 1977, *M.N.R.A.S.*, **181**, 323.
Gott, J. R. 1986, *Nature*, **321**, 420.
Gunn, J. E. 1977, *Ap. J.*, **218**, 592.
Gunn, J. E., and Gott, J. R. 1972, *Ap. J.*, **176**, 1.
Guth, A. H. 1981, *Phys. Rev. D*, **23**, 347.
Hoffman, Y. 1987, *Ap. J.*, submitted.
Hoffman, Y., and Shaham, J. 1985, *Ap. J.*, **297**, 16.
Hogan, C. J. 1987, *Nature*, **326**, 853.
Hogan, C. J., and Rees, M. J. 1984, *Nature*, **311**, 109.
Kaiser, N., and Stebbins, A. 1984, *Nature*, **310**, 391.
Kibble, T. W. B. 1976, *J. Phys. A*, **9**, 1387.
Kormendy, J. 1987, in *IAU Symposium 117, Dark Matter in the Universe*, ed. J. Kormendy and G. R. Knapp (Dordrecht: Reidel), p. 139.
Lin, D. N. C., and Faber, S. M. 1983, *Ap. J. (Letters)*, **266**, L21.
Madsen, J., and Epstein, R. I. 1984, *Ap. J.*, **282**, 11.
Melott, A. L., and Scherrer, R. J. 1987, *Nature*, **328**, 691.
Mészáros, P. 1974, *Astr. Ap.*, **37**, 225.
Ostriker, J. P., Thompson, C., and Witten, E. 1986, *Phys. Letters B*, **180**, 231.
Quinn, P. J., Salmon, J. K., and Zurek, W. H. 1986, *Nature*, **322**, 329.
Sargent, W. L. W., Schechter, P. L., Boksenberg, A., and Shortridge, K. 1977, *Ap. J.*, **212**, 326.
Sato, H. 1986, *Progr. Theor. Phys.*, **75**, 1342.
Schechter, P. 1976, *Ap. J.*, **203**, 297.
Schramm, D. N., and Vittorio, N. 1985, *Comments Nucl. Part. Phys.*, **15**, 1.
Shellard, E. P. S., Brandenberger, R. H., Kaiser, N., and Turok, N. 1987, *Nature*, **326**, 672.
Stebbins, A. 1986, *Ap. J. (Letters)*, **303**, L21.
Traschen, J., Turok, N., and Brandenberger, R. 1986, *Phys. Rev. D*, **34**, 919.
Tremaine, S., and Gunn, J. E. 1979, *Phys. Rev. Letters*, **42**, 407.
Turok, N. 1985, *Phys. Rev. Letters*, **55**, 1801.
Turok, N., and Brandenberger, R. 1986, *Phys. Rev. D*, **33**, 2175.
Vachaspati, T., and Vilenkin, A. 1984, *Phys. Rev. D*, **30**, 2036.
———. 1985, *Phys. Rev. D*, **31**, 3052.
Vilenkin, A. 1981, *Phys. Rev. Letters*, **46**, 1169.
———. 1985, *Phys. Rept.*, **121**, 263.
———. 1986, *Nature*, **322**, 613.
Vilenkin, A., and Shafi, Q. 1983, *Phys. Rev. Letters*, **51**, 1716.
Weinberg, S. 1972, *Gravitation and Cosmology* (New York: Wiley).
White, S. D. M., Frenk, C. S., and Davis, M. 1983, *Ap. J. (Letters)*, **274**, L1.
Witten, E. 1985, *Nucl. Phys. B*, **249**, 557.
Zel'dovich, Ya. B. 1970, *Astr. Ap.*, **5**, 84.
———. 1980, *M.N.R.A.S.*, **192**, 663.
Zurek, W. H. 1986, *Phys. Rev. Letters*, **57**, 2326.

EDMUND BERTSCHINGER: Department of Physics, MIT, 6-207, Cambridge, MA 02139

PAUL N. WATTS: Department of Physics, University of California, Berkeley, CA 94720